Compact modeling of drain current in Independently Driven Double-Gate MOSFETs

D. Munteanu, J.L. Autran*, X. Loussier, O. Tintori

Laboratory for Materials and Microelectronics of Provence, L2MP-CNRS
49 rue Joliot-Curie, 13384 Marseille, France
**Also with Institut Universitaire de France (IUF), Paris, France*
E-mail: daniela.munteanu@l2mp.fr, Phone: +33 4 96 13 98 19, Fax: +33 4 96 13 97 09

ABSTRACT

A compact model for the drain current in Independently Driven Double-Gate (IDDG) MOSFETs is proposed. The model takes into account 2D electrostatics and vertical carrier quantum confinement in the channel. An extensive comparison with numerical data obtained using a full 2D quantum numerical code is performed. The model is shown to fit with a good accuracy numerically simulated quantum drain current in Double-Gate devices with either independent or connected gates.

Keywords: Independently Driven Double-Gate MOSFET, drain current, quantum effects, short-channel effects

1 INTRODUCTION

As CMOS scaling is approaching its limits, Double-Gate (DG) MOSFET is envisaged as a possible alternative to the conventional bulk MOSFET. In spite of excellent electrical performances due to its multiple conduction surfaces, conventional DG MOSFET allows only three-terminal operation because the two gates are tied together. DG structures with independent gates have been recently proposed [1-4], allowing a four terminal operation. Independent Driven Double-Gate (IDDG) devices offer additional potentialities, such as a dynamic threshold voltage control by one of the two gates and transconductance modulation in addition to the conventional switching operation [1, 2]. Modeling the IDDG operation is a difficult task due to the influence of the second gate which can be independently switched. In addition, physical phenomena such as 2D electrostatics or carrier quantization have to be considered for ultra-scaled IDDG structures. In this work, we propose a compact model for the drain current in IDDG, which combines short-channel with quantum confinement effects in the channel. The model is continuous over all operation regimes. A 2-D quantum numerical simulation code [5] (solving the 2D Poisson equation self-consistently coupled with the 1D Schrödinger equation) is used for the model validation. Our model reproduces very well the threshold voltage and the current modulation by the back gate bias, as well as the quantum confinement effects on the inversion charge. It can be directly implemented in a TCAD circuit simulator for the simulation of IDDG based-circuits.

2 DRAIN CURRENT MODELING

Figure 1a shows the schematic of an IDDG structure with and the band diagrams in horizontal and vertical cross-sections are illustrated in Figure 1b and 1c, together with the first energy subbands. The drain current modeling starts with the calculation of the 2D potential distribution in the device. In this work we assume the potential expression given by the equation:

$$\Psi(x,y) = \psi_0(x) + \alpha(x)\left(y - \frac{t_{Si}}{2}\right) + \beta(x)\left(y - \frac{t_{Si}}{2}\right)^2 \quad (1)$$

where Ψ_0 is the potential in the middle of the silicon film. Coefficients α and β are calculated as a function of Ψ_0 using the boundary conditions at the front and the back interfaces between the oxide and the silicon film:

$$E_1 = \frac{\varepsilon_{ox}}{\varepsilon_{Si}} \frac{V_{G1} - V_{FB1} - \psi_{S1}}{t_{ox1}} = -\left.\frac{\partial \psi(x,y)}{\partial y}\right|_{y=0} \quad (2)$$

$$E_2 = \frac{\varepsilon_{ox}}{\varepsilon_{Si}} \frac{V_{G2} - V_{FB2} - \psi_{S2}}{t_{ox2}} = -\left.\frac{\partial \psi(x,y)}{\partial y}\right|_{y=t_{Si}} \quad (3)$$

where V_{FB1} and V_{FB2} are the flat band voltages of the front gate and of the back gate, respectively, $\Psi_{S1}(x)=\Psi(x,y=0)$ and $\Psi_{S2}=\Psi(x,y=t_{Si})$, are the surface potentials at the front and back oxide/film interfaces, respectively. Then, α and β are given by:

$$\alpha = \frac{(V_{FB1} - V_{FB2}) - (V_{G1} - V_{G2})}{t_{Si} + 2\gamma t_{ox}} \quad (4)$$

$$\beta = \frac{V_{G1} - V_{FB1} - \psi_0}{\left(\frac{t_{Si}}{4} + \gamma t_{ox}\right) t_{Si}} + \alpha \frac{\frac{t_{Si}}{2} + \gamma t_{ox}}{\left(\frac{t_{Si}}{4} + \gamma t_{ox}\right) t_{Si}} \quad (5)$$

where $\gamma = \varepsilon_{Si}/\varepsilon_{ox}$. The potential distribution includes the dependence on the front gate and back gate polarizations, V_{G1} and V_{G2}. In equations (4) and (5) we have assumed (for simplification) that $t_{ox1}=t_{ox2}=t_{ox}$. However, this assumption

NSTI-Nanotech 2007, www.nsti.org, ISBN 1420061844 Vol. 3, 2007

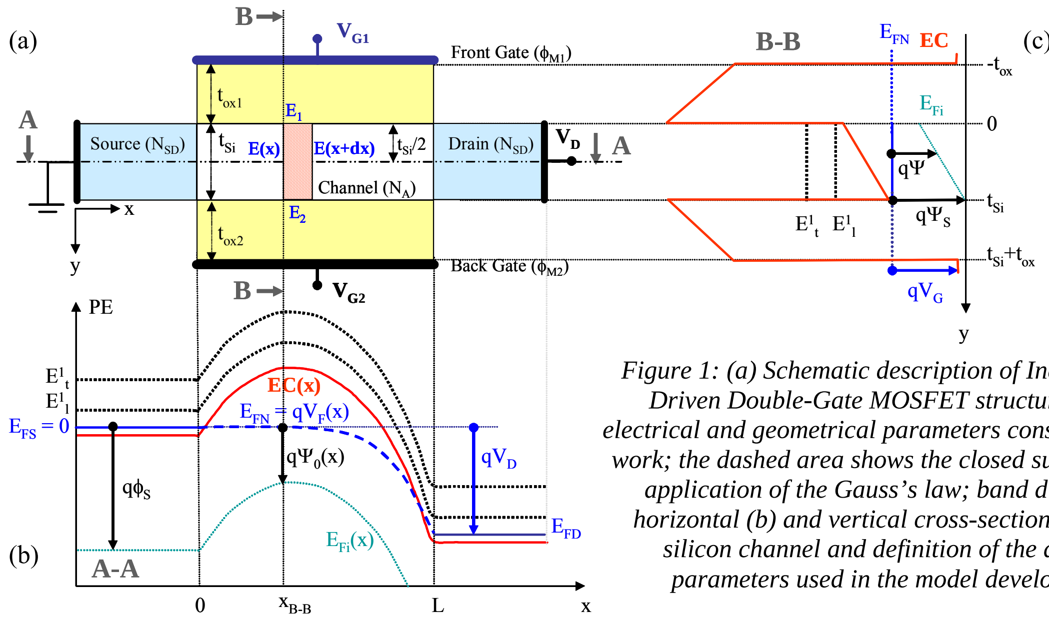

Figure 1: (a) Schematic description of Independently Driven Double-Gate MOSFET structure and its electrical and geometrical parameters considered in this work; the dashed area shows the closed surface for the application of the Gauss's law; band diagram in horizontal (b) and vertical cross-sections (c) in the silicon channel and definition of the different parameters used in the model development.

does not reduce the model generality, since similar development procedure can be applied in the case of front gate oxide and back gate oxide with different thicknesses. For calculating Ψ_0 the Gauss's law is applied to the particular closed dashed surface shown in Figure 1a (as demonstrated in [6, 7]):

$$-\int_0^{t_{Si}} E(x,y)dy + \int_0^{t_{Si}} E(x+dx,y)dy - E_1(x)dx + E_2(x)dx = -\frac{qN_A t_{Si}dx}{\varepsilon_{Si}} - \frac{q_i(x)dx}{\varepsilon_{Si}} \quad (6)$$

In the right hand side, the first term corresponds to the depletion charge (N_A is the channel doping) and the second term is the mobile inversion charge density, given by the integration of the electron charge over the entire Si film. For very thin films used in this work (<15nm), electric field E(x) can be approximated as $E(x) \approx -\frac{d\psi_0(x)}{dx}$. The following differential equation is obtained for Ψ_0:

$$\frac{d^2\psi_0}{dx^2} - m_1^2\psi_0 = R(x) \quad (7)$$

Ψ_0 is then the solution of equation (7) given by:

$$\psi_0(x) = C_1\exp(m_1x) + C_2\exp(-m_1x) - R(x)/m_1^2 \quad (8)$$

where C_1, C_2, R(x) and m_1 are calculated for filling the boundary conditions $\Psi_S(x=0)=\phi_S$ and $\Psi_S(x=L)=\phi_S+V_D$:

$$C_{1,2} = \pm\frac{\phi_S[1-\exp(\mp m_1L)] + V_D + R(0)[1-\exp(\mp m_1L)]/m_1^2}{2\sinh(m_1L)} \quad (9)$$

$$R(x) = \frac{1}{\varepsilon_{Si}t_{Si}C}\times \left(qN_At_{Si} + q_i(x) - 2\varepsilon_{Si}\frac{V_{G1}-V_{FB1}}{t_{Si}/4+\gamma t_{ox}} - 2\alpha\varepsilon_{Si}\frac{t_{Si}/2+\gamma t_{ox}}{t_{Si}/4+\gamma t_{ox}}\right) \quad (10)$$

$$m_1 = \sqrt{\frac{2}{Ct_{Si}(t_{Si}/4+\gamma t_{ox})}}, \quad C = \frac{2}{3}\left(1+\frac{2\gamma t_{ox}}{t_{Si}+4\gamma t_{ox}}\right) \quad (11)$$

$$\phi_S = (kT/q)\ln\left(N_AN_{SD}/n_i^2\right) \quad (12)$$

where N_{SD} is the doping level in the source/drain regions. In equation (10) $q_i(x)$ is the mobile inversion charge density, which can be evaluated in two cases:
(a) the classical case, considering a Boltzmann distribution for the carriers:

$$q_i(x) = \int_0^{t_{Si}} q\,ni\,e^{\frac{q}{kT}[(\psi(x,y)-V_F(x))]}dy \quad (13)$$

(b) the quantum case, where $q_i(x)$ is quantum-mechanically evaluated using the following equation:

$$q_i(x) = \frac{qkT}{\pi\hbar^2}\sum_{l,t}\sum_i m_{2D}^{t,l}g_{t,l}\times \times\ln\left[1+\exp\left(-\beta\left(\tilde{E}^i_{l,t}+\frac{E_g}{2}-\psi_0(x)+V_F(x)\right)\right)\right] \quad (14)$$

where $m^l_{2D} = m^*_t$, $m^t_{2D} = \sqrt{m^*_l m^*_t}$, $m_t^*=0.19\times m_0$, $m_l^*=0.98\times m_0$, $g_l=2$, $g_t=4$, $\beta=q/kT$. In equation (14), $\tilde{E}^i_{l,t}$ are the energy levels calculated using a standard method for first-order perturbation applied to the energy levels of an infinite rectangular well (as shown in [6, 7]):

$$\tilde{E}^i_{l,t} = E^i_{l,t} + \Delta E^i \quad (15)$$

In (15) $E^i_{l,t}$ are the energy levels of an infinite rectangular well given by:

$$E^i_{l,t} = \frac{\hbar^2 \pi^2 i^2}{2 q m^*_{l,t} t^2_{Si}} \quad (16)$$

and $\Delta E^i = \left\langle \varphi^i \middle| H \middle| \varphi^i \right\rangle$, where H is the Hamiltonian of the perturbation and ϕ^i are the electron wave functions associated to energy levels $E^i_{l,t}$.

In equations (13) and (14), $V_F(x)$ is the electron quasi-Fermi level, evaluated by a quasi-empirical expression inspired from [7, 8] and extensively verified by numerical simulation:

$$V_F(x) = \frac{kT}{q} \times \frac{m}{n} \times ln\left[\left(\left(exp\left(\frac{V_D (m/n)^{-1}}{kT/q}\right) - 1\right)\left(\frac{x}{L}\right)^{\frac{c}{(V_{G1}-V_{FB1})+(V_{G2}-V_{FB2})}} + 1\right]^{-1} \times \left(a t_{Si}\right)^{\frac{V_D}{3c}} \quad (17)$$

$m/n = 2 + b\left(V_{G1} - V_{FB1}\right) + b\left(V_{G2} - V_{FB2}\right)$, $a = 0.2\ nm^{-1}$, $b = 0.05\ V^{-1}$, $c = 1\ V^{-1}$. We introduce R(x) given by equation (10) in equation (8). This new expression of $\Psi_0(x)$ is then introduced in equation (14), together with equations (15) and (17). This leads to an implicit equation on $q_i(x)$, which is solved numerically for obtaining $q_i(x)$.

The current density (including both the drift and the diffusion components) is expressed as:

$$J = -q \mu n(x,y) \frac{dV_F(x)}{dx} \quad (18)$$

which is then integrated in the two y and z directions:

$$I_{ds}(x) = \mu W q_i(x) \frac{dV_F(x)}{dx} \quad (19)$$

Current continuity requires $I_{ds}(x)$ be independent of x and integrating (19) in the x direction from 0 to L gives the final expression of the drain current:

$$I_{DS} = \mu \frac{W}{L} \int_0^L q_i(x) dV_F(x) \quad (20)$$

In the case of classical calculation of the inversion charge (i.e. without quantum effects) and considering the Boltzmann distribution for the carriers, the drain current becomes [9]:

$$I_{DS} = \mu \frac{W}{L} \frac{kT}{q} \frac{1 - exp\left(-qV_D / kT\right)}{\int_0^L dy \Big/ \left(\int_0^{t_{Si}} n_i e^{q\psi(x,y)/kT} dx\right)} \quad (21)$$

3 MODEL VALIDATION

The model was validated by an extensive comparison with numerical simulation using a full 2-D Poisson-Schrödinger code [5], adapted for independently driven DG MOSFETs. In a first step, we verified the potential distribution as given by equation (1). In a second step, the classical drain current expression has been validated by numerical simulation, for long channel devices and for film thicknesses from t_{Si}=20nm down to t_{Si}=5nm. We considered a constant mobility in equation (21). Figures 2a and 2b and Figures 3a and 3b show the comparison between the model and numerical simulation in an IDDG MOSFET with L=200nm and t_{Si}=10nm. The drain current characteristics as a function of V_{G1} for both positive and negative V_{G2} (varying from -1.2V to 1.2V with a step of 0.2V) are represented. The fit between the model and the numerical simulation is satisfactory. Figures 2 and 3 illustrate that our model reproduces very well the threshold voltage and the current modulation by the back gate polarization. The investigation of additional $I_D(V_D)$ curves have shown that the model is valid in both linear and saturation regimes. The proposed compact model can easily be used to obtain all main performance indicators of IDDG devices, such as threshold voltage, subthreshold swing, DIBL, I_{on} and I_{off} and their variation as a function of the back gate voltage.

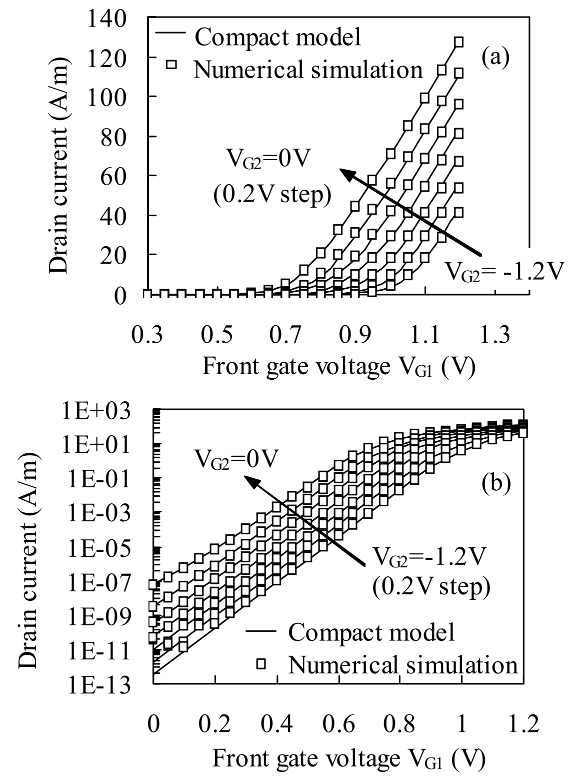

Figure 2: Drain current given by the compact model (classical case) and comparison with numerical simulation in IDDG with t_{Si}=10nm, t_{ox}=1nm and L=200nm. (a) Linear -linear scale and (b) linear-logarithmic scale. V_D=0.1V.

NSTI-Nanotech 2007, www.nsti.org, ISBN 1420061844 Vol. 3, 2007

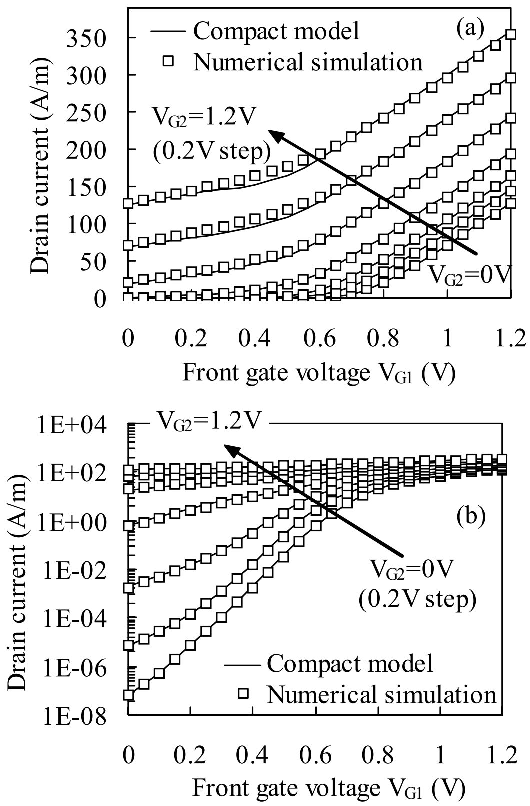

Figure 3: I_D (V_{G1}) for positive back gate voltage for the same device as in Figure 2. (a) Linear-linear scale and (b) linear-logarithmic scale. V_D=0.1V.

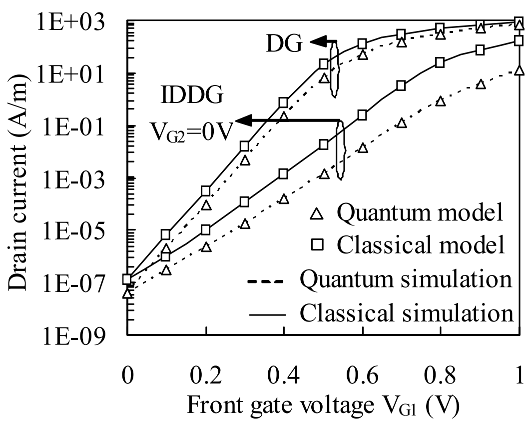

Figure 4: Quantum model verification by numerical simulation in IDDG and DG (connected gates) with t_{Si}=5nm, t_{ox}=1nm and L=50nm. V_D=0.1V.

The validation procedure was continued by an in-depth investigation of the model capability to take into account carrier quantization effects. The quantum drain current as a function of V_{G1} for different V_{G2} values is compared in Figures 4 and 5 with quantum numerical simulation. In Figure 4 the conventional DG structure with connected gates is also considered. A very satisfactory agreement is obtained between the model and the numerical simulation.

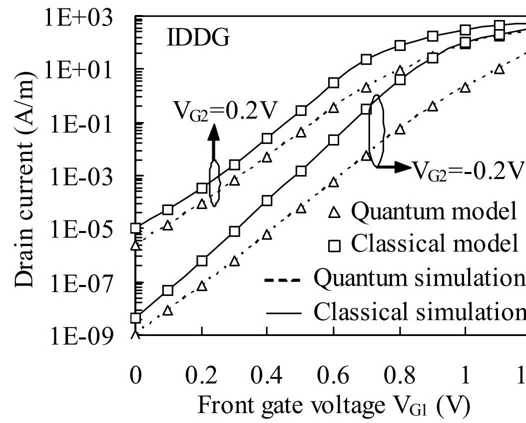

Figure 5: Drain current given by the compact model and comparison with numerical simulation for two values of the back gate voltage in IDDG. The simulated device is the same as in Figure 4.

4 CONCLUSION

We developed a compact model for the drain current in Independently Driven Double-Gate MOSFETs. The model combines 2D electrostatics with vertical quantum confinement effects, which makes it particularly dedicated to ultra-scaled devices expected at the end-of-roadmap. The model is based on an analytical expression of the 2D potential distribution in the channel, taking into account the quantum inversion charge. In order to validate the proposed model, an extensive comparison with quantum numerical simulation using a 2D Poisson-Schrödinger code was performed. The model is shown to reproduce very well the threshold voltage and the current modulation by the back gate polarization, as well as the carrier quantum confinement effects on the drain current.

Acknowledgements

This work was supported by the French Ministry of Research (ANR PNANO project “MULTIGRILLES”).

References

[1] M. Masahara et al., IEEE Trans. Electron Dev., **52** (2005) 2046.
[2] W. Zhang et al., IEEE Trans. Electron Dev., **52** (2005) 2198.
[3] G. Pei and E.C. Kan, IEEE Trans. Electron Dev., **51** (2004) 2086.
[4] G. Pei et al., IEEE Trans. Electron Dev. **50** (2003) 2135.
[5] D. Munteanu, J.L Autran, Solid State Electron., **47**, (2003) 1219.
[6] X. Loussier et al., Nanotech (WCM) 2006, p. 808.
[7] D. Munteanu et al., Molecular Simulation, in press, 2007.
[8] R. van Overstraeten, IEEE Trans. Electron Dev., **22** (1975) 282.
[9] X. Liang, Y. Taur, IEEE Trans. Electron Dev., **51** (2004) 1385.